Chemical Physics 478 (2016) 48–54

Contents lists available at ScienceDirect

Chemical Physics

journal homepage: www.elsevier.com/locate/chemphys

Charge transport properties of a twisted DNA molecule: A renormalization approach

M.L. de Almeida [a], G.S. Ourique [a], U.L. Fulco [a], E.L. Albuquerque [a,*], F.A.B.F. de Moura [b], M.L. Lyra [b]

[a] Departamento de Biofísica e Farmacologia, Universidade Federal do Rio Grande do Norte, 59072-970 Natal-RN, Brazil
[b] Instituto de Física, Universidade Federal de Alagoas, 57072-900 Maceió-AL, Brazil

ARTICLE INFO

Article history:
Available online 4 June 2016

Keywords:
Tight-binding Hamiltonian
Renormalization approach
Twisted DNA segment
Electronic transmittance spectra
I × V characteristic curves

ABSTRACT

In this work we study the charge transport properties of a nanodevice consisting of a finite segment of the DNA molecule sandwiched between two metallic electrodes. Our model takes into account a nearest-neighbor tight-binding Hamiltonian considering the nucleobases twist motion, whose solutions make use of a two-steps renormalization process to simplify the algebra, which can be otherwise quite involved. The resulting variations of the charge transport efficiency are analyzed by numerically computing the main features of the electron transmittance spectra as well as their I × V characteristic curves.

1. Introduction

Due to the increase diversification of materials requiring specific electronic properties, nowadays research in charge transport has been changing its focus from solid-state crystals to organic molecules [1–3]. One of the main reason for that is the use of different physical and biochemical methods on important biological polymers, since the approaches to these molecules should be fundamentally different from those working for any other inorganic or non-bioorganic substance. As a consequence, their structural and dynamical behavior is much more complicated than that either artificial polymers or conventional materials. The net result is the recognition of novel functional materials surpassing in many ways the conventional ones, as well as unraveling their novel and important mechanisms [4–7].

The transmission and conduction processes of the DNA charge transport between two conductors electrodes is a challenger structural problem associated not only to the design and construction of such junctions, but also to the need to understand their macroscopic transport properties, the output being the transformation of structural DNA nanotechnology to practical applications as an important component in nano-electronic devices. Indeed, basic properties pertaining to single electron transistor behavior and to current rectification of a molecular device made up of an oligopeptide chain directly coupled to two platinum electrodes have already been demonstrated [8]. More intriguing still, and a challenge for biochemists today, is the consideration of the consequences and opportunities for charge transport through the DNA base pair stack within the cell.

A variety of experimental approaches have been used to probe the charge transport in biological molecules, mainly those related with DNA and proteins, a scientific advance bridging the molecular world to the world where we live. In particular, earliest studies involved physical measurements of current flow in DNA segments lead to a mixture of conclusions, some suggesting high electron mobility, while others indicating opposite conclusions [9–12]. Some years ago, the conductivity of DNA duplexes bridging a carbon nanotube gap have been measured. The observed resistance through stacked DNA bases was found to be comparable to the resistance perpendicular to graphite planes [13]. More recently, experiments on DNA charge transport in 100-mer monolayers on gold have demonstrated an efficient transport over distances as large as 34 nm [14], thus exceeding that of most reports of molecular wires. As a result, charge transport in biological molecule has triggered recently a series of theoretical and experimental investigations (for a recent review see [15] and the references there in).

Theoretical models devised to study the electronic transport in DNA molecules assume that the transmission channels are along their longitudinal axis. A π-stacked array of DNA nucleobases, formed by a symbolic sequence of a four letters alphabet, namely guanine (G), adenine (A), cytosine (C) and thymine (T), provides the way to promote long-range charge migration, which in turn gives important clues about the mechanisms and biological

* Corresponding author.
E-mail address: eudenilson@gmail.com (E.L. Albuquerque).

http://dx.doi.org/10.1016/j.chemphys.2016.05.020
0301-0104/

functions of charge transport [16–20]. Based on these previous works and the related literature, there is a vast collection of possible theoretical mechanisms to provide electronic transport in DNA (or low-dimensional molecules). A central point to emphasize is that DNA is a low-dimensional disordered structure and therefore, the electronic eigenfunctions become exponentially localized due to the scattering by the intrinsic disorder (Anderson localization). Some authors proposed that internal DNA correlations could be relevant to promote charge transport. Although the presence of long-range correlations within the disorder distribution in DNA can in fact increase the electronic localization length, it has been shown that it does not have a significant impact on the localized nature of the states [21,22]. However, the distinct character of the intrinsic base pair correlations in coding and non-coding DNA segments has been shown to produce measurable differences in the electronic properties of intron and exon-like segments [23].

Usually charge transfer studies for a wide variety of systems, including organic materials such as the DNA molecule, are based on the Schrödinger equation in the tight-binding approximation for both random and quasiperiodic sequences of the on-site potential ϵ_n and/or the hopping potential t_{nm} between the quantum states $|n\rangle$ and $\langle m|$, the former (latter) leading to Anderson localization (Cantor set of zero Lebesgue measure). Focusing on the DNA case, the model consider a simplified vision of the Watson–Crick pairs attached to the sugar-phosphate backbone condensed into a single nucleotide site. Although it was successful employed to describe numerous experimental data [15], it has some critical assessment, as discussed by Shinwari et al. [24]. One key point is the "one-orbital-per-site" picture, insufficient in some aspect to characterize the quantum state. A reasonable solution is the adoption of nucleotide pairs instead of the separate nucleotides to define the tight-binding quantum states by using more sophisticated quantum chemistry models such as the DFT (Density Functional Theory) approach, whose accuracy is achieved at a greater computer cost. Other relevant consideration is the topology of the double-helix, which is not a rigid object, with the different constituents of DNA moving relative to each other presenting linear deformations of its structure in response to the charge arrival at this particular site (polaronic effects), beyond the scope of the present work. The presence of water molecules and counterions interacting with the nucleobases and the backbone can be taken into account by considering a realistic value of the backbone ionization energy. Fortunately, we do not expect any relevant change by considering these refinements in our tight-binding model, keeping the main features of our results unaffected.

In this work, we use a model Hamiltonian within a two-steps renormalization approach to describe the charge transport properties of a twisted DNA molecule following the model described in [25,26]. Our description of the DNA molecule takes into account the contributions of the nucleobase system as well as the sugar-phosphate backbone molecules on a tight-binding Hamiltonian model. The DNA's helicoidal structure is considering by means of not only the longitudinal intra-chain hopping term but also the twist angle $\theta_{n,n\pm1}$ between two adjacent base pair $(n, n\pm1)$ attached along the molecule backbone. The resulting variations of the charge transport efficiency are analyzed by numerically computing the main features of their transmittance and I × V characteristic curves.

This paper is organized as follows: in Section 2 we present our theoretical approach based on a tight-binding model Hamiltonian solved by the help of a two-steps renormalization process. Section 3 deals with the discussion of the charge transfer properties, by means of the electronic transmittance spectra and the current–voltage (I × V) characteristic curves. The conclusions and perspective of future works are depicted in Section 4.

2. Theoretical model

We use a tight-binding model Hamiltonian to describe the charge transport properties of a DNA molecule sandwiched by two metallic electrodes (the source−S and the drain−D contacts), considered to be platinum, with a single orbital per site and nearest-neighbor interactions (see Fig. 1a). Our description of the DNA molecule takes into account the contributions of the nucleobase system, considering both the base pairing between the complementary strands and the stacking interaction between nearest-neighbor bases, as well as the sugar-phosphate backbone, yielding:

$$H_{total} = H_{DNA} + H_{electrode} + H_{coupling}. \tag{1}$$

Here, the first term H_{DNA} describes the inter and intra-strand charge propagation through the DNA molecule, the second term $H_{electrode}$ is related to the two metallic electrodes, while the last term $H_{coupling}$ describes the coupling between the DNA strand and the semi-infinite metallic electrodes.

A relevant feature to be considered here is the inclusion of torsional effects, responsible for the helicoidal DNA structure. This effect was already considered in earlier works [27–31]. Its role is quite important since in physiological conditions the DNA's double helix structure exhibits a full-fledged three-dimensional geometry. As a consequence, every two consecutive nucleobases are twisted by a certain angle $\theta_{n,n\pm1}$ (in equilibrium conditions $\theta_{n,n\pm1} = \theta_0 = \pi/5$), and therefore the orbital overlapping is substantially reduced, yielding smaller values for the hopping integral values [32,33]. In addition, at physiological temperatures the relative orientation of neighboring bases becomes a function of time, thereby modifying their mutual overlapping in an oscillatory way (dynamical effect). Twisted DNA model was also considered [34,35] using a path integral formalism to study the thermodynamics of a short fragment of heterogeneous DNA interacting with a stabilizing solvent on the temperature range in which denaturation takes place.

Considering the nucleobases as identical point masses, helically arranged and mutually connected by means of elastic rods, which describe the sugar-phosphate backbone, the position of the nth nucleobase can be expressed in cylindrical coordinates as

$$x_n = r_n \cos\phi_n, \quad y_n = r_n \sin\phi_n, \quad z_n = r_0\phi_n, \tag{2}$$

where n labels the considered base-pair along the DNA double strand, r_n and ϕ_n are the usual cylindrical coordinates, and $r_0 = h_0/\theta_0, h_0 \approx 0.34$ nm being the equilibrium separation between two successive base-pair planes (B-DNA form). Thus, the geometrical distance between two neighboring nucleobases can be expressed as [31]

$$d_{n,n\pm1} = \left[r_0^2\theta_{n,n\pm1}^2 + r_n^2 + r_{n\pm1}^2 - 2r_n r_{n\pm1}\cos\theta_{n,n\pm1}\right]^{1/2}, \tag{3}$$

where, $\theta_{n,n\pm1} = \pm\phi_{n+1} \mp \phi_n$. In equilibrium conditions

$$d_{n,n\pm1} = l_0 = \left[h_0^2 + 4r_n^2\sin^2(\theta_0/2)\right]^{1/2}. \tag{4}$$

Following the procedure described in Refs. [32,31], and considering that the atomic orbitals are orthogonal to each other, in the equilibrium condition ($d_{n,n\pm1} = l_0$) the full 3D description of the helix geometry yields, for the longitudinal intra-chain hopping term:

$$t_L(\theta_{n,n\pm1}) = t_L(\theta_t) = t_L(0)\left[1 - \eta\left(\frac{2r_0}{l_0}\sin\frac{\theta_{n,n-1}}{2}\right)^2\right]. \tag{5}$$

Here

$$\eta = 1 + |\eta_{pp\pi}|/\eta_{pp\sigma}, \tag{6}$$

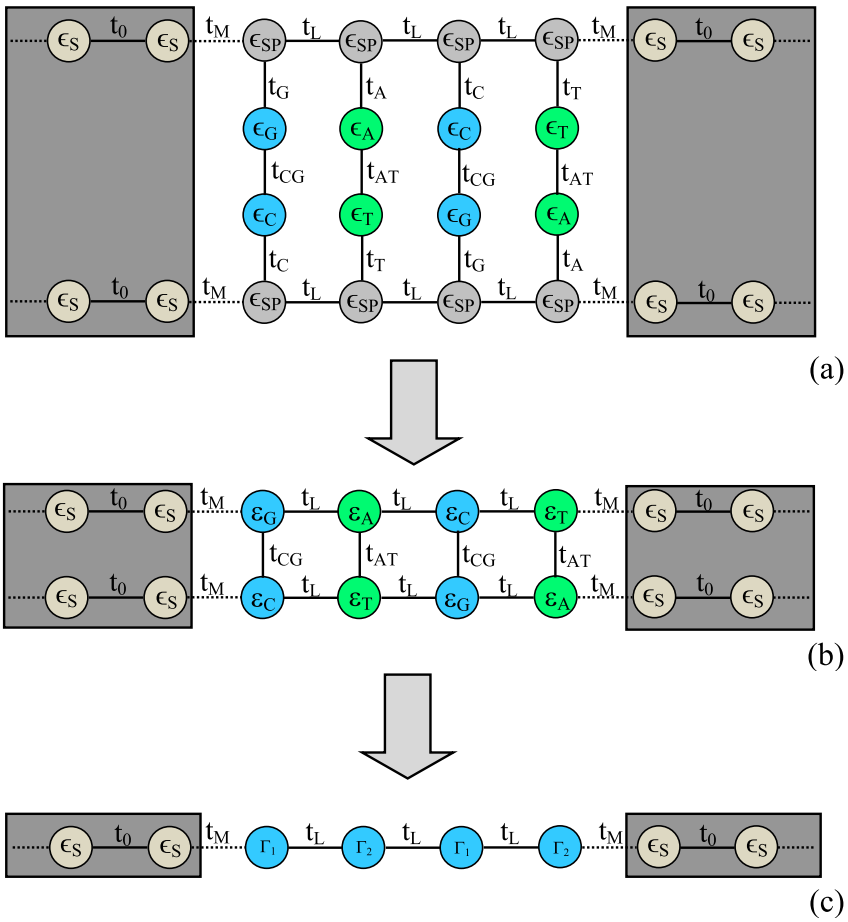

Fig. 1. Sketch illustrating the renormalization process mapping the DNA chain model (a), first into a linear diatomic lattice (b), and then a linear monoatomic lattice (c), reducing the eleven physical parameters, namely, the ionized energies ϵ_{SP} (sugar-phosphate backbone) and ϵ_α (α being the four nitrogen bases A, T, C, G), and the hopping terms t_α (between the nitrogen bases and the sugar-phosphate backbone) and $t_{\alpha\beta}$ (the transverse hopping between the nitrogen bases), into three variables only, the hopping term t_L (the longitudinal hopping between the nitrogen bases) and the ionized energies $\Gamma_j(E)$ ($j = 1, 2$).

where $\eta_{pp\pi}$ and $\eta_{pp\sigma}$ describe the hibridization matrix elements between neighboring bases p_z orbitals [32]. Further simplification can be done, if one considers the propagation of low-frequency twist oscillations (acoustic modes), leading to a small (although non-zero) fixed twist angle θ_t, i.e.:

$$t_L(\theta_t) = t_L(0)(1 - \chi\theta_t^2). \tag{7}$$

Here, χ is a dimensionless coupling strength between the charge and the lattice system. For small twists, $\chi = 2.92$ [31].

In order to get a simple mathematical description of the DNA molecule, keeping most of its relevant physical information, we use now a two-steps renormalization process. In the first step we mapped the full DNA chain into a linear diatomic lattice (see Fig. 1b). Afterwards, we renormalize the linear diatomic lattice into a one-dimensional lattice shown in Fig. 1c, reducing the eleven physical parameters, namely:

(a) the ionized energies ϵ_{SP} (sugar-phosphate backbone) and ϵ_α (α being the four nitrogen bases A, T, C, G);
(b) the hopping terms t_α (between the nitrogen bases and the sugar-phosphate backbone) and $t_{\alpha\beta}$ (the transverse hopping between the nitrogen bases).

into three variables only, the hopping term t_L (the longitudinal hopping between the nitrogen bases) and the ionized energies $\Gamma_j(E)$ ($j = 1, 2$), defined by:

$$\Gamma_1(E) = t_{CG} + \sum\nolimits_{\alpha=C,G} \frac{\tau_\alpha^2(E)}{E - \epsilon_{SP}}, \tag{8}$$

with

$$\tau_\alpha(E) = t_\alpha + \frac{\epsilon_\alpha(E - \epsilon_{SP})}{t_\alpha}, \quad \alpha = C, G. \tag{9}$$

The term $\Gamma_2(E)$ can be obtained from Eqs. (8) and (9), provided we replaced C, G by A, T.

The energies ϵ_α are chosen from the ionization potential of their respective bases. Taking into account explicitly the contribution of water molecules, their experimental values are [36–40]: ϵ_A = 7.7 eV (adenine), ϵ_T = 8.1 eV (thymine), ϵ_G = 7.4 eV (guanine), and ϵ_C = 8.1 eV (cythosine). We use the energy of the electrode (platinum) ϵ_M = 5.36 eV, which is related to the work function of this metal [41]. The energy of the sugar-phosphate backbone is ϵ_{SP} = 12.27 eV, justified by the presence of a number of counterions and water molecules, located along the DNA backbone structure, interacting with the nucleobases and the backbone itself by means of hydration, solvation, and charge transfer processes [25]. We take the hopping potentials between the base (G, C, A or T) and the sugar-phosphate (SP) backbone as $t_G = t_C = t_A = t_T$ = 1.0 eV, while the hopping between the base pair intra (inter)-chain is $t_L(0) = 0.15$ eV ($t_{GC} = 0.9$ eV and $t_{AT} = 0.3$ eV, respectively) [25], which are within the range of values obtained by quantum

chemistry calculations [42]. Furthermore, the hopping term in the electrode is t_0 = 12.0 eV [43].

Now considering the renormalization procedure depicted schematically in Fig. 1, the first term of the Hamiltonian (1) is described by

$$H_{DNA} = \sum_{j=1,2}\sum_{n}\Gamma_j(E)|n><n| + \sum_{n} t_L(\theta_t)|n><n\pm 1|. \tag{10}$$

The second term, related to the two semi-infinite metallic electrodes, reads:

$$H_{electrode} = \sum_{n=-\infty}^{0}[\epsilon_M|n><n| + t_0|n><n\pm 1|] + \sum_{n=N+1}^{\infty}[\epsilon_M|n><n| + t_0|n><n\pm 1|], \tag{11}$$

where $\epsilon(M)$ (t_0) is the ionized energy (hopping term) of the electrode. Our DNA molecule is coupled to the electrodes by the tunneling Hamiltonian

$$H_{coupling} = t_M[|0><1| + |N><N+1|], \tag{12}$$

where $t_M = 0.63$ eV represents the hopping amplitude between the source (drain) electrode and the beginner (end) of the DNA base-pair structure, N being the number of nucleotides in the structure under consideration [44].

3. Results and discussions

Considering the tight-binding Hamiltonian given above, the transmission coefficient $T_N(E)$, that gives the transmission rate through the chain and is related to the Landauer resistance, is defined by [21]

$$T_N(E) = \frac{4 - X^2(E)}{[-X^2(E)(\mathcal{P}_{12}\mathcal{P}_{21}+1) + X(E)(\mathcal{P}_{11}-\mathcal{P}_{22})(\mathcal{P}_{12}-\mathcal{P}_{21}) + \sum_{i,j=1,2}\mathcal{P}_{ij}^2 + 2]}, \tag{13}$$

where

$$X(E) = \left[E - \sum_{j=1,2}\Gamma_j(E)\right] \Big/ t_L(\theta_t), \tag{14}$$

and $\mathcal{P}_{ij}$ are elements of the transfer-matrix $\mathcal{P} = M(N)M(N-1)\cdots M(2)M(1)$, with [45]

$$M(j) = \begin{pmatrix} X(E) & -1 \\ 1 & 0 \end{pmatrix}. \tag{15}$$

For a given energy E, $T_N(E)$ measures the level of backscattering events in the electrons (or hole) transport through the chain.

Fig. 2 depicts the transmittance spectra as a function of the energy (less the Fermi energy) in units of eV, for the Poly GC sequence, in which $\Gamma_1(E) \neq 0$ and $\Gamma_2(E) = 0$ (Fig. 2a), Poly AT sequence, in which $\Gamma_1(E) = 0$ and $\Gamma_2(E) \neq 0$ (Fig. 2)b, and Poly GCAT sequence in which $\Gamma_1(E)$ and $\Gamma_2(E)$ are different of zero (Fig. 2c). We have considered the Fermi energy equal to the guanine's ionization energy for the Poly GC and Poly GCAT structures, and adenine's for the Poly AT one. Also N, the number of nucleotides, is equal to 24, and the torsion angle $\theta_t = 0$ (black full line) and $\pi/10$ (blue full line). The transmittance spectra show several energies with high transmission resonances [$T_N(E) = 1$], besides a striking symmetry around the energies 1.71 (Poly GC, see Fig. 2a), 1.46 (Poly AT, see Fig. 2b) and 1.21 (Poly GCAT, see Fig. 2c), all units in eV, independent of the value of the torsion angle θ. The reason for the former (symmetrical spectra) is due to the periodicity of the DNA structures considered here, as depicted in Fig. 1, since for quasi-periodic DNA structure the energy spectra exhibit distinct physical properties, giving rise to a novel description of disorder. Indeed, theoretical transfer matrix treatments can be used to show that these spectra are fractals, defining intermediate systems between a periodic and a random structure [46]. The independence on the torsion angle θ lies on the role played by the sugar-phosphate backbone ionization energy ϵ_{SP}. Indeed, the expected two transmission bands around the ionization energies of the Guanine-ϵ_G and Cytosine-ϵ_C (Adenine-ϵ_A and Thymine-ϵ_C) basis for the Poly GC (Poly AT) structure, formed when the backbone ionization energy ϵ_{SP} is equal to zero, progressively approach each other as ϵ_{SP} increases, leading to the one band structure depicted in Figs. 2,a 2,b and 2c for its realistic value considered here [47]. This profile is insensitive to the adopted value for the hydrogen bonding strength ($t_{GC} = 0.9$ eV and $t_{AT} = 0.3$ eV, respectively) responsible for the binding of the complementary DNA strands, because its energetic value is much less than the backbone ionization energy ϵ_{SP} = 12.27 eV, justified by the presence of a number of counterions and water molecules.

It is important to mention that stationary electron transmission spectra through finite DNA chains is usually investigated throughout a dynamical map, as it is quite common in quasi-periodic systems. According to that, the electronic transmission properties present localization of the electronic wave functions, in despite of the fact that long-range correlations in DNA finite segments could be a possible mechanism to induce delocalization. However, the actual correlations are not strong enough to produce this correlation-induced transition and the stationary states remain all localized [21,22]. For inhomogeneous random sequences, the scenario is worst since almost all states are strongly localized and the electronic transport is dominated by dissipative processes. Nevertheless, as in our case, the presence of long-range correlations due to the periodicity of the renormalized structure might enhance the localization length and, therefore, the transmission resonances survive in larger segments as compared with a non-correlated random sequence.

The transmission coefficient $T_N(E)$ is a useful quantity to describe the transport efficiency in quantum systems. Nonetheless, $T_N(E)$ is usually difficult to be directly measured experimentally. Access to transmission properties can be performed by measuring their I × V characteristics by applying the Landauer-Büttiker formulation [48,49], i.e.:

$$I(V) = \frac{2e}{h}\int_{-\infty}^{+\infty} T_N(E)[f_S(E) - f_D(E)]dE, \tag{16}$$

where $f_{S(D)}$ is the Fermi–Dirac distribution given by:

$$f_{S(D)} = \left[\exp[(E-\mu_{S(D)})/k_BT] + 1\right]^{-1}. \tag{17}$$

Here $\mu_{S(D)}$ is the electrochemical potential of the two electrodes fixed by the applied bias voltage V as $|\mu_S - \mu_D| = eV$. Before that, the electrochemical potential of the whole system is taken to be zero. It must be kept in mind, however, that the determination of the electronic properties of biological molecules such as DNA segments, should be done taking into account a transport theory considering the time evolution of the appropriate charge propagation, as depicted in Eq. 1. The reason for that is because static solid-state theory is not capable of capturing all aspects of the charge transfer dynamics in biomolecules.

As V is switched on, by properly locating the Fermi level energy equal to the lowest characteristic resonances of the electrode-DNA molecule-electrode nano-junction, namely guanine for the Poly GC and Poly GCAT structures, and adenine for the Poly AT one, the transmission coefficient becomes voltage-dependent leading to the appearance of transmission band shifts. As a result, the I × V

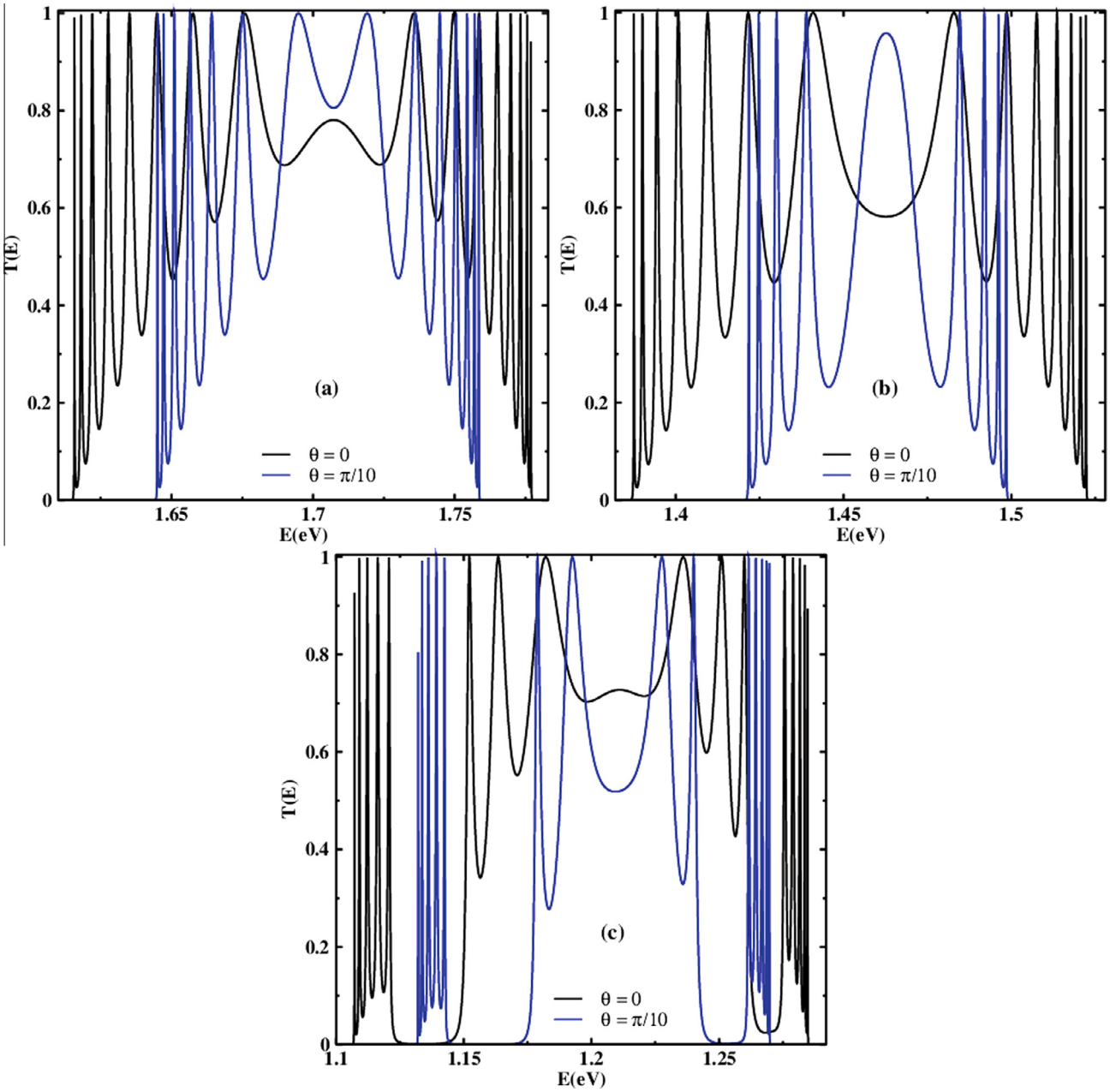

Fig. 2. Transmittance spectra as a function of the energy (less the Fermi energy, which is equal to the guanine's ionization energy for the Poly GC and Poly GCAT structures, and adenine's for the Poly AT one) in units of eV considering N (the number of nucleotides) equal to 24, and a torsion angle $\theta_t = 0$ (black full line) and $\pi/10$ (blue full line). (a) DNA Poly GC; (b) DNA Poly AT; (c) DNA Poly GCAT. (For interpretation of the references to colour in this figure caption, the reader is referred to the web version of this article.)

curves may show a current rectification due to the appearance of either a lower or a higher current at a given bias [8]. Nonetheless, the turn-on current here shows a symmetric profile, with either none or a negligible rectification current, as depicted in Figs. 3a (Poly GC), 3b (Poly AT) and 3c (Poly GCAT) for several torsion angles.

Fig. 3a shows the Poly GC current–voltage profiles for torsion angles $\theta_t = 0$ (black full line), $\theta_t = \pi/30$ (red full line), $\theta_t = \pi/15$ (green full line) and $\theta_t = \pi/10$ (blue full line). All of them present an ohmic region $-2.5\ \text{V} \leqslant V \leqslant 2.5\ \text{V}$, and symmetric regions otherwise, indicating a semiconductor behavior which can be attributed to the resonant dipoles of the DNA segment leading to an overall depletion region effect. This behavior can be explained by the tunneling of electrons under an energy barrier between adjacent localized states of the basis so that electrons can travel through the molecule mainly by the hopping mechanism. The localized states may be located in the vicinity of the Fermi energy of the electrodes, so that when voltage bias is applied, the Fermi energy alignes with a localized state and the charge electron transport is initiated. No rectifying behavior is observed indicating that the charge transport in the highest occupied molecular orbital (HOMO) of the Poly GC DNA, located at the guanine base, is of the same magnitude of its lowest unoccupied molecular orbital (LUMO), located at the cytosine base, when the voltage bias is applied to the sample. It is worth mentioning that the observed symmetry might be contaminated by a residual Schottky effect from the contacts, as measured by the contribution of $H_{electrode}$ depicted in Eq. 11. The maximum value of the current, obtained when there is no torsion angle, is 8.26 μA. Observe that as the torsion angle θ_t increases, the absolute value of the current decreases indicating a transition towards an

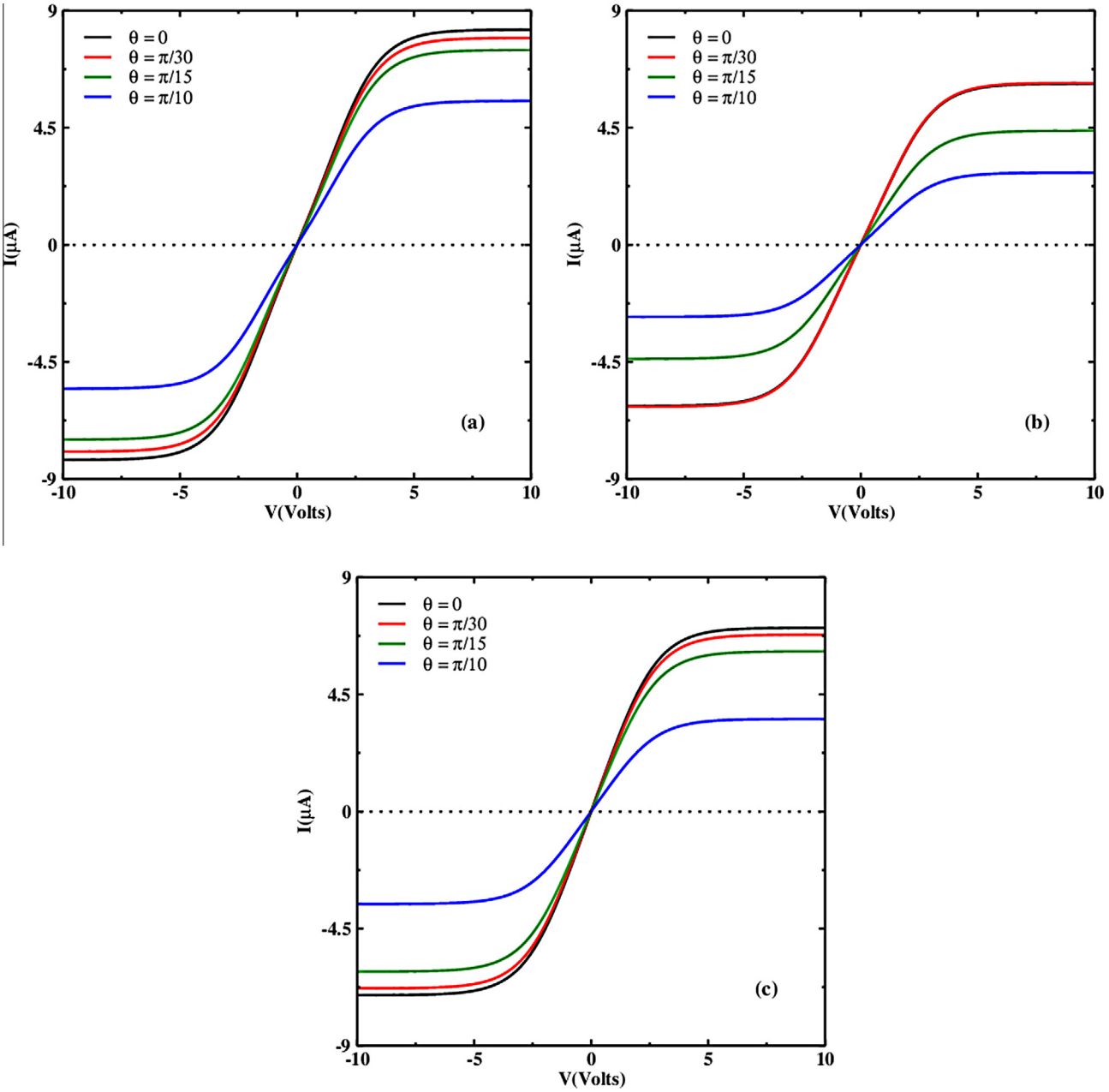

Fig. 3. I × V characteristic curves for torsion angles θ_t = 0 (black full line), $\theta_t = \pi/30$ (red full line), $\theta_t = \pi/15$ (green full line) and $\theta_t = \pi/10$ (blue full line). (a) DNA Poly GC; (b) DNA Poly AT; (c) DNA Poly GCAT. (For interpretation of the references to colour in this figure caption, the reader is referred to the web version of this article.)

insulator phase, reaching a critical value at θ_t approximately equal to $\pi/7.5$ (Poly GC); $\pi/7$ (Poly AT) and $\pi/6.2$ (Poly GCAT), all of them below the torsion angle $\theta_t = \pi/5$ between the base pairs of the B-form of DNA [50].

Fig. 3b (3c) shows a similar pattern for the Poly AT (Poly GCAT) current–voltage profiles for the same torsion angles. Observe that for the Poly AT case the curve without torsion angle (θ_t = 0, black full line), is hidden by the red curve corresponding to $\theta_t = \pi/30$. The maximum value of the current, is now 6.20 (7.06) μA.

4. Conclusions

In conclusion, by using an effective tight-binding model, we have theoretically investigated the transport properties of a molecular device made up of a DNA double-helix molecule, including the sugar-phosphate contribution, directly coupled to two platinum electrodes. The electronic transmittance and I × V characteristics are discussed in terms of its on-site ionization and electrode energies, as well as its different hopping parameters. Overcoming the limitations modeling the DNA trough two parallel chains, we have also introduced a twist angle θ_t between two adjacent base pair attached along the molecule backbone. In order to get a simple mathematical description of the DNA molecule, keeping most of its relevant physical information, we used also a two-steps renormalization process to map it into a linear monoatomic lattice, allowing us to incorporate the sugar-phosphate backbone contribution into an energy-dependent on-site ionization potential on the main DNA's basepairs.

Future works in this field should point to the possibility of developing new sophisticated nanodevices integrating man-made nanostructures with different biomolecules, as well as the above mentioned DNA base pair stack within the cell. In doing so, care

should be taken with the DNA's spontaneous point mutations, whose plausible cause is the so-called rare tautomers arising from the proton transfer (PT) reactions between the base pairs double helix architecture of DNA proposed by Watson and Crick [51]. Nano biomolecular sensors may be developed for the detection of these point structural defects in DNA associated with the formation of the mismatches of the canonical A-T and G-C Watson–Crick base pairs [52–54]. Our $I \times V$ characteristic curves, depicted in Fig. 3, may shed some light on this biologically important question, in the same line as those developed in a previous work [55]. Another important mechanism, besides the biological environment, is the vibrational modes and the formation of polarons (the bound state of an electron with a lattice distortion). Surely they might open up the possibility of monitoring and controlling critical biological functions and processes in unprecedented ways, giving rise to a vast array of potential technological achievements.

Acknowledgments

This work was partially financed by the Brazilian Research Agency CAPES (PNPD) and CNPq (INCT-Nano(Bio) Simes and Casadinho/Procad).

References

[1] A.L. Furst, Michael G. Hill, J.K. Barton, Langmuir 31 (2015) 6554.
[2] A.L. Furst, S. Landfield, M.G. Hill, J.K. Barton, J. Am. Chem. Soc. 135 (2013) 19099.
[3] K. Göpfrich, T. Zettl, A.E.C. Meijering, S. Hernández-Ainsa, S. Kocabey, T. Liedl, U.F. Keyser, Nano Lett. 15 (2015) 3134.
[4] J.A. McCammon, S. Harvey, Dynamics of Proteins and Nucleic Acids, Cambridge University Press, Cambridge, 1987.
[5] N.C. Seeman, Annu. Rev. Biophys. Biomol. Struct. 27 (1998) 225.
[6] H.-A. Wagenknecht (Ed.), Charge Transfer in DNA: From Mechanism to Application, Wiley, New York, 2005.
[7] G. Cuniberti, E. Maciá, A. Rodriguez, R.A. Römer, in: T. Chakraborty (Ed.), Charge Migration in DNA: Perspectives from Physics, Chemistry and Biology, Springer, Berlin, 2007.
[8] J.I.N. Oliveira, E.L. Albuquerque, U.L. Fulco, P.W. Mauriz, R.G. Sarmento, Chem. Phys. Lett. 612 (2014) 14.
[9] D. Porath, A. Bezryadin, S. De Vries, C. Dekker, Nature 403 (2000) 635.
[10] B. Xu, P. Zhang, X. Li, N. Tao, Nano Lett. 4 (2004) 1105.
[11] R.G. Sarmento, E.L. Albuquerque, P.D. Sesion Jr, U.L. Fulco, B.P.W. de Oliveira, Phys. Lett. A 373 (2009) 1486.
[12] L.M. Bezerril, D.A. Moreira, E.L. Albuquerque, U.L. Fulco, E.L. de Oliveira, J.S. de Sousa, Phys. Lett. A 373 (2009) 3381.
[13] X. Guo, A.A. Gorodetsky, J. Hone, J.K. Barton, C. Nuckolls, Nat. Nanotechnol. 3 (2008) 163.
[14] J.D. Slinker, N.B. Muren, S.E. Renfrew, J.K. Barton, Nat. Chem. 3 (2011) 228.
[15] E.L. Albuquerque, U.L. Fulco, V.N. Freire, E.W.S. Caetano, M.L. Lyra, F.A.B.F. de Moura, Phys. Rep. 535 (2014) 139.
[16] F.A.B.F. de Moura, M.L. Lyra, E.L. Albuquerque, J. Phys.: Condens. Matter 20 (2008) 075109.
[17] C.M. Chang, A.H. Castro Neto, A.R. Bishop, Chem. Phys. 303 (2004) 189.
[18] E. Diaz, F. Dominguez-Adame, Chem. Phys. 365 (2009) 24.
[19] F.A.B.F. de Moura, U.L. Fulco, M.L. Lyra, F. Doínguez-Adame, E.L. Albuquerque, Phys. A 390 (2011) 535.
[20] M.O. Sales, U.L. Fulco, M.L. Lyra, E.L. Albuquerque, F.A.B.F. de Moura, J. Phys.: Condens. Matter 27 (2015) 035104.
[21] E.L. Albuquerque, M.S. Vasconcelos, M.L. Lyra, F.A.B.F. de Moura, Phys. Rev. E 71 (2005) 021910.
[22] E.L. Albuquerque, M.L. Lyra, F.A.B.F. de Moura, Phys. A 370 (2006) 625.
[23] A.A. Krokhin, V.M.K. Bagci, F.M. Izrailev, O.V. Usatenko, V.A. Yampolskii, Phys. Rev. B 80 (2009) 085420.
[24] M.W. Shinwari, M.J. Deen, E.B. Starikov, G. Cuniberti, Adv. Funct. Mater. 20 (2010) 1865.
[25] E. Maciá, Phys. Rev. B 74 (2006) 245105.
[26] R.G. Sarmento, U.L. Fulco, E.L. Albuquerque, E.W.S. Caetano, V.N. Freire, Phys. Lett. A 375 (2011) 3993.
[27] K. Drukker, G. Wu, G.C. Schatz, J. Chem. Phys. 114 (2001) 579.
[28] A. Campa, Phys. Rev. E 63 (2001) 021901.
[29] M. Barbi, S. Lepri, M. Peyrard, N. Theodorakopoulos, Phys. Rev. E 68 (2003) 061909.
[30] J. Palmeri, M. Manghi, N. Destainville, Phys. Rev. Lett. 99 (2007) 088103.
[31] E. Maciá, Phys. Rev. B 76 (2007) 245123.
[32] R.G. Endres, D.L. Cox, R.R.P. Singh, Rev. Mod. Phys. 76 (2004) 195.
[33] A. Voityuk, J. Jortner, M. Bixon, N. Rösch, J. Chem. Phys. 114 (2001) 5614.
[34] M. Zoli, J. Chem. Phys. 135 (2011) 115101.
[35] M. Zoli, J. Chem. Phys. 138 (2013) 205103.
[36] A. Muñoz-Losa, D. Markovitsi, R. Improta, Chem, Phys. Lett. 634 (2015) 20.
[37] H. Fernando, G.A. Papadantonakis, N.S. Kim, P.R. Lebreton, Proc. Nat. Acad. Sci. U.S.A. 95 (1998) 5550.
[38] C. Yu, T.J. Odonnell, P.R. Lebreton, J. Phys. Chem. 85 (1981) 3851.
[39] J. Lin, C. Yu, S. Peng, I.K. Akiyama, L.I. Li Kao Lee, P.R. LeBreton, J. Phys. Chem. 84 (1980) 1006.
[40] H.B. Schlegel, J. Chem. Phys. 84 (1986) 4530.
[41] Y-A. Berlin, A.L. Burin, M.A. Ratner, Chem. Phys. 275 (2002) 61.
[42] A. Voityuk, J. Jortner, M. Bixon, N. Roesch, J. Chem. Phys. 114 (2002) 5614.
[43] E. Maciá, F. Triozon, S. Roche, Phys. Rev. B 71 (2005) 113106.
[44] G. Cuniberti, L. Craco, D. Porath, C. Dekker, Phys. Rev. B 65 (2002) 241314.
[45] P.W. Mauriz, E.L. Albuquerque, M.S. Vasconcelos, Phys. A 294 (2001) 403.
[46] E.L. Albuquerque, M.G. Cottam, Polaritons in Periodic and Quasiperiodic Structures, Elsevier, Amsterdam, 2004.
[47] E. Maciá, S. Roche, Nanotechnology 17 (2006) 3002.
[48] R. Landauer, IBM, J. Res. Dev. 1 (1957) 223.
[49] M. Büttiker, Phys. Rev. B 35 (1987) 4123.
[50] M. Egli, W. Saenger, Principles of Nucleic acid Structure, Springer, New York, 1984.
[51] P.O. Löwdin, Rev. Mod. Phys. 35 (1963) 724–732.
[52] J.P. Cerón-Carrasco, D. Jacquemin, Phys. Chem. Chem. Phys. 17 (2015) 7754–7760.
[53] O.O. Brovarets, R.O. Zhurakivsky, D.M. Hovorun, J. Comp. Chem. 35 (2014) 451–466.
[54] O.O. Brovarets, D.M. Hovorun, Phys. Chem. Chem. Phys. 16 (2014) 15886–15899.
[55] L.M. Bezerril, U.L. Fulco, J.I.N. Oliveira, G. Corso, E.L. Albuquerque, V.N. Freire, E. W.S. Caetano, Appl. Phys. Lett. 98 (2011) 053702.